ASME Letters in Dynamic Systems and Control. Received November 01, 2024;
Accepted manuscript posted May 8, 2025. doi:10.1115/1.4068615

Josefredo G. da Silva[1]
Centre for Ocean Energy Research,
Department of Electronic Engineering,
Maynooth University,
Maynooth, Co. Kildare, Ireland
email: josefredo.silva.2024@mumail.ie

Márcio J. Lacerda
Centre for Communications Technology,
School of Computing and Digital Media,
London Metropolitan University,
London, UK
email: m.lacerda@londonmet.ac.uk

Ariadne L. J. Bertolin
Department of Mechanical Engineering,
University of Bath,
Bath, United Kingdom
email: adljb20@bath.ac.uk

Thalita Nazaré
Centre for Ocean Energy Research,
Department of Electronic Engineering,
Maynooth University,
Maynooth, Co. Kildare, Ireland
email: thalita.nazare.2023@mumail.ie

Matheus Costa
Centre for Ocean Energy Research,
Department of Electronic Engineering,
Maynooth University,
Maynooth, Co. Kildare, Ireland
email: matheus.costa.2024@mumail.ie

Erivelton Nepomuceno
Hamilton Institute,
Centre for Ocean Energy Research,
Department of Electronic Engineering,
Maynooth University,
Maynooth, Co. Kildare, Ireland
email: erivelton.nepomuceno@mu.ie

H_∞ Control Co-design for Uncertain Polytopic Systems

Control Co-design (CCD) refers to approaches that fully integrate plant and control system interactions, using an optimisation-based methodology where physical and control system designs are addressed simultaneously. In this process, the design of physical systems and their controllers are typically interdependent tasks. This study explores a bi-level(nested) control co-design approach integrated with robust H_∞ control for the combined design of both the physical system and its controller. While the nested approach is well-established in the literature, with the linear quadratic regulator commonly used for controller optimisation, this work introduces a novel approach by focusing on minimising the H_∞ norm/guaranteed cost as the controller optimisation problem instead. The proposed method seeks to bridge the fields of control co-design and robust control, extending the application of control co-design to systems subject to disturbances and parametric uncertainties. It assumes that any uncertain system parameter can be described as a subset of a polytopic domain, and that a feedback-stabilising control can be synthesised to ensure the H_∞ norm/guaranteed cost of the system is bounded, thus minimising the impact of exogenous inputs on the system's output. The synthesis conditions are demonstrated through linear matrix inequalities and an adaptation of traditional Lyapunov stability conditions. To illustrate the method presented, this study revisits two previously addressed control co-design problems in the literature: a scalar plant and an active car suspension system. The results indicate that the integration of CCD with robust control strategies not only guarantees system performance and disturbance rejection but also provides a systematic approach for managing uncertainties within a polytopic framework.

Keywords: Control Co-design, H_∞ norm/guaranteed cost, Parametric Uncertainties, Linear Matrix Inequalities, Robust Control

1 Introduction

Control Co-design (CCD) refers to approaches that fully integrate plant and control system interactions, using an optimisation-based methodology where physical and control system designs are addressed simultaneously [1]. This method aims to harness the interaction between the physical system (plant) and the control system design to maximise system performance [2]. Traditional methodologies typically involve the sequential design of various domains within a plant, with the controller design concluding the process. However, this conventional approach can lead to sub-optimal performance in systems where there is significant coupling between the controller and plant dynamics. Therefore, the design of physical systems should incorporate control design considerations [3].

It has been stated that CCD, along with model reduction techniques, is key to the future of control systems when considering collaborative efforts in design processes [4]. Additionally, CCD has been applied to a variety of systems recently, demonstrating that it is possible to achieve higher performance by designing the plant and control systems concurrently. In previous work, the applications of CCD in engineering and technology fields have been reviewed [5]. It has been demonstrated that key areas of extensive application and growing interest include renewable energy [6], particularly technologies related to offshore energy generation [7–10], for which significant computational tools have been developed [11]. Additionally, this includes, but is not limited to, autonomous and electric vehicles [12,13], aircraft systems [14], drones [15], robotics [1,15], and other cyber-physical systems [16].

The concept of CCD is closely linked to established engineering practices related to optimisation-based methodologies that focus on integrated design approaches: Engineers frequently need to modify and adapt systems to meet specific requirements, especially when integrating control design alone is insufficient. These modifications typically aim to meet requirements at a minimised cost.

In this sense, formal methodologies have been developed to identify potential plant modifications while minimising costs through co-design approaches [17]. For example, Allison and Herber introduce Multidisciplinary Design Optimisation (MDO) [3], a field that investigates design methods for systems involving multiple disciplines, as a reorganisation of the optimisation problem

[1]Corresponding Author.
Version 1.18, March 19, 2025

ASME Letters in Dynamic Systems and Control. Received November 01, 2024;
Accepted manuscript posted May 8, 2025. doi:10.1115/1.4068615

based on the plant and control disciplines. Allison, Guo, and Han [18] introduce Direct Transcription (DT) as a method for co-design, illustrating its application in an automotive active suspension system. Iterative sequential methods have also been proposed [19]. Plant-Limited Co-Design (PLCD) was introduced as a methodology for identifying potential plant modification candidates through the use of CCD, with the goal of minimising the cost of these modification [20]; among others. However, considering the various methodologies through which CCD has been studied, to the best of the authors' knowledge, there is a lack of works that relate CCD to polytopic systems subject to disturbances. Since uncertainties and disturbances are common challenges that control systems must address, and polytopic systems provide an effective way to model these uncertainties, integrating polytopic systems within the CCD framework could be a robust approach to tackling the uncertainty problem in CCD applications.

Uncertainties and disturbances in control systems often arise from unknown dynamics, unidentified high-frequency components, parameter estimation inaccuracies, sensor and actuator errors, and system nonlinearities. These factors can lead to deviations from the desired system behaviour. In addition, model uncertainty significantly imposes new challenges for control design, as the controller must satisfy control specifications across a range of uncertain parameters, rather than for a plant with precisely known characteristics. Examining a control solution independently for each possible plant configuration within the uncertainty range is referred to as a brute-force approach, which is highly time-consuming and may even be impractical [21]. Therefore, methods that, unlike adaptive control, can design a single fixed controller capable of simultaneously handling multiple performance specifications, such as noise/disturbance rejection, reference tracking, and stability, are of utmost importance.

By modelling uncertain parameters within a polytopic domain and applying stability arguments from Lyapunov theory, we can derive stability and control design conditions in the form of Linear Matrix Inequalities (LMIs). The LMIs can be easily written and solved using Semi-definite Programming Algorithms (SDP) such as YALMIP [22] and SeDuMi [23]. Additionally, thanks to the convex properties of the polytopic description, the LMIs can be checked by using the vertices of the polytope. This method has been broadly applied in robust control theory [24–28]. However, the use of this technique for CCD still needs to be explored further.

As CCD involves adapting an existing system's design and controller in tandem to meet new task requirements, it is typically associated with the concept of optimality. In this context, optimal control plays a crucial role. For example, Fathy et al. utilise a CCD approach known as nested CCD. In this method, established optimal control formulations are applied in an inner loop to address control optimality for each plant design candidate generated by an outer loop, while the plant's outer loop optimises the system-level objective using a controller that is optimal for the plant [29]. Allison and Nazari, on the other hand, use augmented Lagrangian coordination to address system optimality [30]. Another significant aspect of control design, as highlighted by Allison, Guo, and Han [18], is that the optimal open-loop control problem can sometimes be employed in the early stages of design, with the assumptions regarding a specific control architecture addressed later. In this approach, feedback is regarded as a secondary step, where control design variables are used to parameterise a feedback control law. In this later stage, classical optimal control methods, such as the Linear Quadratic Regulator (LQR), are well recognised.

While the significance of applying LQR in CCD applications is widely acknowledged [31], and combining optimal control with the Karush-Kuhn-Tucker (KKT) conditions [32] and/or Pontryagin's Minimum Principle (PMP) [33] is a common strategy for ensuring optimality within a CCD framework [17,31], robust control strategies are often employed for systems affected by uncertainties and disturbances, with H_∞ control being one of the most traditional methods. The aim of H_∞ control is to reduce the impact of uncertainties and disturbances, helping the system maintain its performance and stability despite unpredictable variations. Therefore, for these kind of systems replacing LQR with H_∞ control could enhance system performance and may even be considered novel, given the existing gap in the literature on CCD frameworks that address these systems.

The selection of H_∞ as the control strategy in this work was driven by its robustness to uncertainties and modelling inaccuracies. Since CCD inherently involves iterative procedures across a range of values for both physical and control parameters—often subject to approximations and uncertainties—it was deemed appropriate to integrate a CCD approach with a control strategy renowned for its ability to handle uncertainties and modelling errors. Additionally, unlike LQR, which relies on the selection of only two Hermitian positive-definite matrices (Q and R) and often requires a trial-and-error tuning process, H_∞ provides greater flexibility in defining control decision variables through LMI-based formulations.

As CCD applications generally involve iterating through multiple plant/controller candidates until an optimal solution is found. While H_∞ control typically minimises the effects of disturbances in sequential approaches for precisely known systems, an important question remains: how does the H_∞ norm/guaranteed cost of a system respond to parameter changes within a CCD framework? In other words, the impact of optimisation routines that continuously update physical parameters on the H_∞ norm/guaranteed cost of a system is yet to be fully explored.

To approach these questions, this study explores a CCD approach integrated with robust H_∞ control for the combined design of physical systems and their controllers, specifically focusing on uncertain, continuous, linear, time-invariant (LTI) systems subject to disturbances. The methodology in the present work assumes that uncertain system parameters can be represented within a polytopic domain, allowing for the synthesis of a feedback-stabilising control that ensures the boundedness of the H_∞ norm/guaranteed cost, thus also ensuring optimality. Two necessary conditions for certifying closed-loop stability are presented in terms of linear matrix inequalities (LMIs), using Lyapunov theory. These conditions have been applied in prior work to certify the stability of uncertain LTI systems affected by disturbances [34,35]. Although these conditions have already been explored in the literature, there remains potential to apply them within the CCD framework. Thus, rather than developing new synthesis conditions, the main contribution of this paper is to bridge the fields of CCD and robust control, extending CCD applications to systems subjected to disturbances and parametric uncertainties while formulating the CCD problem in a polytopic context.

To illustrate the proposed method, this study revisits two control co-design problems previously addressed in the literature: a scalar plant and an active car suspension system. The scalar plant case is a simple example of a precisely known system, but it is highly relevant in the context of CCD. In contrast, the active suspension case explores the methodology presented in this work more extensively, as it involves a system modelled with uncertain parameters and is subject to disturbances.

Section 2 presents the formulation adopted for describing parameter uncertainty as a set of a polytopic domain, and different CCD approaches present in literature. Section 3 presents the formulation of LMI conditions for synthesising robust output feedback gains for continuous-time uncertain linear systems, along with the formalism of the bi-level (nested) CCD approach adopted in this paper. Section 4 consists of numerical examples that apply the method presented in Section 3 to a scalar plant and an active car suspension. In this section, the physical model, mathematical model, and control co-design framework are described. Finally, Section 5 offers the conclusions.

2 Preliminaries

In this section, the foundational concepts for systems with uncertainty, modelled within a polytopic domain, are introduced, along-

ASME Letters in Dynamic Systems and Control. Received November 01, 2024;
Accepted manuscript posted May 8, 2025. doi:10.1115/1.4068615

side the definition of H_∞ guaranteed cost and key optimisation approaches, to support understanding and practical application within co-design.

2.1 Systems Modelled with Parametric Uncertainties. Consider the linear continuous time-invariant system with uncertainties, described by the following set of equations:

$$\begin{cases} \dot{\xi}(t) = A(\alpha)\xi(t) + B(\alpha)u(t) + B_w(\alpha)w(t), \\ z(t) = C_z(\alpha)\xi(t) + D_{zu}(\alpha)u(t) + D_{zw}(\alpha)w(t), \end{cases} \tag{1}$$

where $\xi \in \mathbb{R}^n$ is the state vector, $u \in \mathbb{R}^{n_u}$ is the control input vector, $w \in \mathbb{R}^{n_w}$ represents the disturbance input and $z \in \mathbb{R}^{n_z}$ is the controlled output. The matrices $A(\alpha) \in \mathbb{R}^{n\times n}, B_w(\alpha) \in \mathbb{R}^{n\times n_w}, B(\alpha) \in \mathbb{R}^{n\times n_u}$, $C_z(\alpha) \in \mathbb{R}^{n_z\times n}, D_{zw}(\alpha) \in \mathbb{R}^{n_z\times n_w}$, and $D_{zu}(\alpha) \in \mathbb{R}^{n_z\times n_u}$ belong to a polytopic domain and can be represented in terms of their vertices such as

$$\Xi(\alpha) = \sum_{i=1}^{N} \alpha_i \Xi_i, \tag{2}$$

where Ξ_i represents each vertex of the polytope and $\Xi(\alpha)$ can represent any of the uncertain matrices of the system (1). Moreover, the parameter α belongs to the unit simplex [36,37] of dimension N denoted by

$$\Lambda_N = \left\{ \alpha \in \mathbb{R}^N : \sum_{i=1}^{N} \alpha_i = 1, \alpha_i \geq 0, \text{ for } i = 1, \dots, N \right\}, \tag{3}$$

a precisely known system can be determined from Eq. (1), since the set defined in Eq. (3) is assumed to have dimension $N = 1$. In this case, for simplicity of notation $\Xi(\alpha)$ is denoted simply by Ξ.

Consider a state-feedback control law $u = K\xi$, where $K \in \mathbb{R}^{n_u\times n}$ is the control gain. The closed-loop system reads

$$\begin{cases} \dot{\xi}(t) = A_{cl}\xi(t) + B_w(\alpha)w(t), \\ z(t) = C_{z,cl}\xi(t) + D_{zw}(\alpha)w(t), \end{cases} \tag{4}$$

where $A_{cl} = A(\alpha) + B(\alpha)K$, and $C_{z,cl} = C_z(\alpha) + D_{zu}(\alpha)K$.

2.2 H_∞ Norm/Guaranteed cost. For the system in Eq. (1), the H_∞ norm/guaranteed cost can be defined as the maximum value derived from the ratio between the energy of the output signals, $z(t)$, and the disturbance input signal, $w(t)$, for all $w(t) \in \mathcal{L}_2$, i.e., the set of signals with finite energy [38].

$$\|H_{wz}\|_\infty = \max_{w(t)\in\mathcal{L}_2} \frac{\|z(t)\|_2}{\|w(t)\|_2}, \quad w \neq 0,$$

Assuming that the referred system is internally stable, and $\|H_{wz}\|_\infty < \gamma$, for a certain $\gamma \in \mathbb{R}$, $\gamma > 0$, then $\int_{t_0}^{t} \left(\|z(\tau)\|_2 - \gamma^2\|w(\tau)\|_2\right) d\tau \leq 0, \quad \forall \quad w(t) \in \mathcal{L}_2, \quad \forall \quad t \geq t_0$ [39].

Let $w(t)$ be an exogenous input and $z(t)$ the controlled output; minimising the H_∞ norm/guaranteed cost corresponds to minimising the energy influence of the exogenous input on the controlled output. The H_∞ norm/guaranteed cost is closely related to frequency-domain analysis tools such as the Bode diagram and the singular value plot. In a single-input single-output (SISO) system, the Bode magnitude plot provides insight into the worst-case gain over all frequencies, which directly connects to the H_∞ norm/guaranteed cost as the peak value of the system's transfer function. In multi-input multi-output (MIMO) systems, the singular value plot generalises this concept by representing the frequency-dependent gain through the largest singular value of the transfer function matrix. Thus, minimising the H_∞ norm/guaranteed cost ensures that the system's worst-case response is controlled across all input disturbances, making it a crucial performance metric in robust control design.

Lastly, from an interpretability perspective, the H_∞ norm/guaranteed cost provides an upper bound on the system's energy amplification, allowing its role to be intuitively understood in terms of power attenuation and stability margins. A lower H_∞ norm/guaranteed cost corresponds to reduced sensitivity to disturbances, which translates into improved robustness and potential energy savings in practical implementations. This connection highlights its relevance as a practical measure of performance, particularly when direct visualisation through Bode or singular value plots is not available.

2.3 Control Co-design Formulations. Fathy et al. [31] define combined plant/controller optimisation strategies, as illustrated in Fig. 1, and classify them into four different strategies: sequential, iterative, simultaneous, and bi-level (nested). In a sequential approach, the plant is designed first, followed by the controller. The iterative method typically relies on LMIs, where, given an initial plant/controller design, an iterative optimisation process is defined. This process improves the plant without compromising the controller, then optimises the controller and repeats this process over multiple iterations. On the other hand, the bi-level strategy involves two nested loops, with the outer loop focusing on plant optimisation and the inner loop on controller optimisation. Lastly, the simultaneous strategy optimises both the plant and controller concurrently.

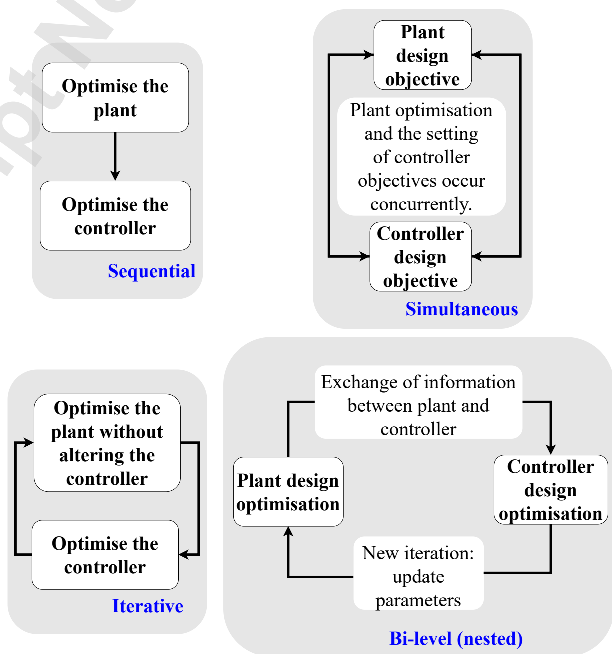

Fig. 1 A typical sequential plant/controller design compared with three common CCD approaches: iterative, bi-level (nested), and simultaneous. ***Source: elaborated by the authors.***

For a more detailed comparison of various optimisation strategies in CCD, refer to [17], where the authors examine the differences between nested and simultaneous approaches. This study emphasises several aspects of the nested strategy, particularly the notion that, although the simultaneous approach is regarded as the most fundamental way to represent an integrated design problem, the nested method restructures the optimisation process by distinguishing between the plant and control disciplines. Additionally, it

ASME Letters in Dynamic Systems and Control. Received November 01, 2024;
Accepted manuscript posted May 8, 2025. doi:10.1115/1.4068615

naturally deals with bidirectional coupling, although it is typically known for being computationally expensive.

To illustrate this point, Alison, Guo, and Han [18] implemented both the simultaneous and nested approaches, comparing them to the traditional sequential design in an active car suspension case study. While the simultaneous approach using DT demonstrated superior performance, the results for the nested method were omitted in the cited paper, as it was deemed highly computationally inefficient. This omission, however, leaves room for further exploration of the nested approach, particularly in combination with frameworks that optimise computational efficiency.

The literature presents examples where the nested approach has demonstrated superior results [40,41], while in other cases, the simultaneous method has shown better performance [18]. Therefore, the selection of these approaches may depend on the specific application. Consequently, it is valuable to provide literature-based recommendations across various case studies to assess different CCD approaches [1,42].

Cui, Alison, and Wang conducted a study integrating CCD with Reliability-Based Design Optimisation (RBDO) [43]. Their work assessed non-deterministic co-design strategies and included a comparative study of RBDO algorithms, as well as the integration of simultaneous and nested CCD approaches within RBDO formulations. It is highlighted the importance of nested formulation when dealing with multidisciplinary problems, which reduces the complexity of decoupled sub-problems. Separating the optimal control design and reliability evaluation from the initial problem increases flexibility in selecting solution algorithms. By using specialised algorithms for each sub-problem, it is possible to achieve overall benefits, particularly by lowering the computational expense of solving the inner loop. In this sense, we consider the nested CCD approach to be the most suitable for the present study, as it provides greater flexibility in the separation of physical and control system design, aligning with our objective of developing a more adaptable framework.

2.4 Bounded Real Lemma. This subsection introduces the Bounded Real Lemma (BRL) [44], an essential result in robust control theory that connects the characterisation of a system's H_∞ performance to a set of state-space-based matrix inequalities. By providing conditions under which the H_∞ norm of a LTI system remains bounded, the BRL facilitates both theoretical analysis and practical controller synthesis, ensuring specific performance levels in the presence of disturbances and uncertainties. It also clarifies how system properties such as stability and detectability influence robust performance, and supports various optimisation-based approaches in modern control system design.

Lemma 1. *Consider the system given by Eq. (1), if there exist matrices $P = P' > 0$, and Z, such that*

$$\min_{Z,P=P'>0} \mu$$

$$\begin{bmatrix} AP + PA' + BZ + Z'B' & PC_z' + Z'D_{zu}' & B_w \\ C_zP + D_{zu}Z & -\mu\mathbf{I} & D_{zw} \\ B_w' & D_{zw}' & -\mathbf{I} \end{bmatrix} < 0. \tag{5}$$

then the referred system is exponentially stable, and the feedback gain, $K = ZP^{-1}$, ensures that $\|H(s)\|_\infty \leq \sqrt{\mu}$, $\mu \in \mathbb{R}$ [44].

Proof. $\|H_{wz}(s)\|_\infty < \gamma$ implies that $\|z(t)\|_2 \leq \gamma\|w(t)\|_2$, $w(t) \in \mathcal{L}_2$. Equivalently, $z(t)'z(t) \leq \gamma^2 w(t)'w(t)$ or $z(t)'z(t) - \gamma^2 w(t)'w(t) \leq 0$. For a system characterised by a matrix A that is bounded and continuous, let $V(t,\xi) = \xi' P \xi$, a Lyapunov function, where $P = P' > 0$. It holds that

$$\begin{aligned} &\dot{V}(\xi) + z(t)'z(t) - \gamma^2 w(t)'w(t) < 0 \Rightarrow \\ &\dot{\xi}' P\xi + \xi' P\dot{\xi} + z'z - \gamma^2 w'w < 0, \end{aligned} \tag{6}$$

by substituting (1) into (6), one gets:

$$\begin{aligned} &(A\xi + Bu + B_w w)' P\xi + \xi' P(A\xi + Bu + B_w w) \\ &+(C_z\xi + D_{zu}u + D_{zw}w)'(C_z\xi + D_{zu}u + D_{zw}w) \\ &-\gamma^2 w'w < 0, \end{aligned} \tag{7}$$

simplifying and rearranging the terms in (7) gives:

$$\begin{bmatrix} \xi \\ w \end{bmatrix}' \begin{bmatrix} A'P + PA + C_z'C_z & PB_w + C_z'D_{zw} \\ B_w'P + D_{zw}'C_z & D_{zw}'D_{zw} - \gamma^2 I \end{bmatrix} \begin{bmatrix} \xi \\ w \end{bmatrix} < 0. \tag{8}$$

The inequality (8) can be rewritten as:

$$\begin{bmatrix} A'P + PA & PB_w \\ B_w'P & -\gamma^2 I \end{bmatrix} - \begin{bmatrix} C_z' \\ D_{zw}' \end{bmatrix} \begin{bmatrix} -I \end{bmatrix} \begin{bmatrix} C_z & D_{zw} \end{bmatrix} < 0, \tag{9}$$

applying the Schur complement to (9) leads to

$$\begin{bmatrix} A'P + PA & PB_w & C_z' \\ B_w'P & -\gamma^2\mathbf{I} & D_{zw}' \\ C_z & D_{zw} & -\mathbf{I} \end{bmatrix} < 0. \tag{10}$$

For the controller synthesis, a feedback gain $K \in \mathbb{R}^{m\times n}$ is determined such that the control law $u(t) = K\xi(t)$ minimises the H_∞ norm and asymptotically stabilises the system in Eq. (1). The closed-loop dynamic and output matrices are $A_{cl} = A + BK$, and $C_{z,cl} = C_z + D_{zu}K$, respectively, and the closed-loop transfer function (TF) between the input $w(t)$ and the output $z(t)$ is given by

$$H_{wz}(s) = (C_z + D_{zu}K)(sI - (A + BK))^{-1}B_w + D_{zw}, \tag{11}$$

For precisely known systems, the primal and dual strategies provide the same results for computing stabilising gain and H_∞ norm [44]. From inequality (10), one can determine the equivalent BRL for a dual system related to the system described in Eq. (1), and subjected to the control law $u(t) = K\xi(t)$:

$$\begin{bmatrix} A_{cl}P + PA_{cl}' & PC_{z,cl}' & B_w \\ C_{z,cl}P & -\gamma^2\mathbf{I} & D_{zw} \\ B_w' & D_{zw}' & -\mathbf{I} \end{bmatrix} < 0 \tag{12}$$

replacing $A_{cl} = A + BK$ and $C_{z,cl} = C_z + D_{zu}K$ in (12) gives:

$$\begin{aligned} &\begin{bmatrix} (A+BK)P + P(A+BK)' & P(C_z + D_{zu}K)' & B_w \\ (C_z + D_{zu}K)P & -\gamma^2 I & D_{zw} \\ B_w' & D_{zw}' & -I \end{bmatrix} < 0 \Rightarrow \\ &\begin{bmatrix} AP + PA' + BZ + Z'B' & PC_z' + Z'D_{zu}' & B_w \\ C_zP + D_{zu}Z & -\mu I & D_{zw} \\ B_w' & D_{zw}' & -I \end{bmatrix} < 0 \end{aligned} \tag{13}$$

where $Z = KP$, and $\mu = \gamma^2$, which makes the combined search for the stabilising gain K and the Lyapunov matrix P a convex problem and concludes the proof. □

3 Main Results

This section describes the CCD formulation used in this paper and introduces Lemma 2, which characterises the H_∞ performance of general continuous-time polytopic LTI systems. A finite set of LMIs, defined at the polytope vertices, is provided to obtain a feedback gain that ensures system stabilisation when the exogenous input is zero, and establishes an H_∞ upper bound on system performance when the exogenous input is non-zero. This new condition alleviates the conservatism of the approach presented in Lemma 1 and circumvents non-convex formulations of the optimisation problem by introducing additional slack variables into the LMI control design procedure.

ASME Letters in Dynamic Systems and Control. Received November 01, 2024;
Accepted manuscript posted May 8, 2025. doi:10.1115/1.4068615

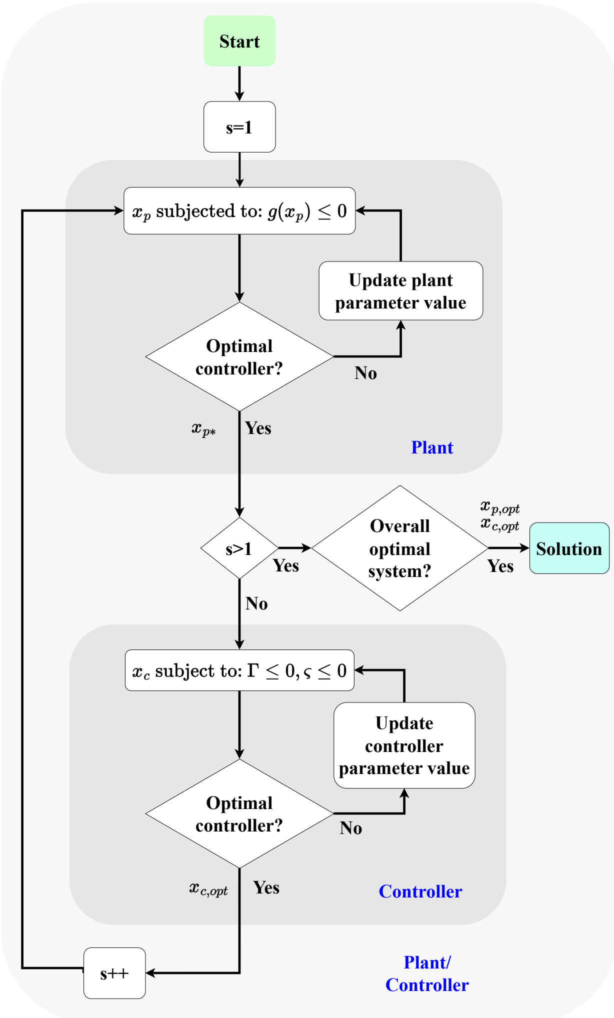

Fig. 2 A bi-level CCD approach. A physical parameter is selected based on the plant constraints, and the H_∞ value is initially computed. This process continues until the physical parameter that minimises the H_∞ value is identified. The optimisation is then repeated, keeping the previously determined value of the plant fixed, while adjusting the controller parameters to find an optimal solution. Finally, after the control parameters that optimise the controller cost are found, the plant values are iterated again, with the controller values kept fixed, until the optimal solution is identified. *Source: elaborated by the authors.*

Lemma 2. *Consider the system given by Eq. (1), if there exist matrices $P = P' > 0$, G, Z, H, and scalar β such that*

$$\min_{Z,G,H,\beta,P=P'>0} \mu$$

$$M = \begin{bmatrix} A(\alpha)G + G'A(\alpha)' + B(\alpha)Z + Z'B(\alpha)' & \star & \star & \star \\ P - G + \beta(A(\alpha)G + B(\alpha)Z)' & M_{22} & \star & \star \\ C_z(\alpha)G + D_{zu}(\alpha)Z & M_{32} & -\mu\mathbf{I} & \star \\ -H'B_w(\alpha)' & 0 & -H'D_{zw}(\alpha)' & \mathbf{I} + H + H' \end{bmatrix} < 0, \quad (14)$$

with, $M_{22} = \beta(G + G')$, and $M_{32} = \beta(C_z(\alpha)G + D_{zu}(\alpha)Z)$. Then the referred system is exponentially stable and, the state feedback gain $K = ZG^{-1}$ stabilises the system with a guaranteed cost $\|H_{wz}\|_\infty \le \sqrt{\mu}$, $\mu \in \mathbb{R}$, $\forall \alpha \in \Lambda$.

Proof. Let's us consider the following congruence transformation

$$T = \begin{bmatrix} \mathbf{I} & A_{cl}(\alpha) & 0 & B_w(\alpha) \\ 0 & C_{z,cl}(\alpha) & \mathbf{I} & D_{zu}(\alpha) \end{bmatrix} \quad (15)$$

where, $A_{cl}(\alpha) = A(\alpha) + B(\alpha)K$, and $C_{z,cl}(\alpha) = C_z(\alpha) + D_{zu}(\alpha)K$. By replacing the expression for the feedback gain, $K = ZG^{-1}$ one gets:

$$A_{cl}(\alpha)G = A(\alpha)G + B(\alpha)Z \quad (16)$$

$$C_{z,cl}(\alpha)G = C_z(\alpha)G + D_{zu}(\alpha)Z \quad (17)$$

By applying the congruence transformation in Eq. (15) to the LMI (14), such that $\tilde{M} = T'MT$, along with a Schur complement, and substituting Eqs. (16) and (17), holds

$$\begin{bmatrix} A_{cl}(\alpha)P + PA_{cl}(\alpha)' & PC_{z,cl}(\alpha)' & B_w(\alpha) \\ \star & -\gamma^2\mathbf{I} & D_{zw}(\alpha) \\ \star & \star & -\mathbf{I} \end{bmatrix} < 0 \quad (18)$$

which corresponds to the dual version of the BLR, as presented in Eq. (13), thus concluding the proof. □

It is worth noting that the conditions presented in this paper do not guarantee convergence of the optimisation problem for the control-synthesis LMIs. While the plant and control constraints will be chosen from a practical feasibility standpoint (refer to the following sections), no analytical proofs have been provided to ensure that the LMI variables always lie within a feasible region. Additionally, no extensive computational validation will be performed. Hence, the proposed conditions serve only as *sufficient*, rather than *necessary*, conditions for the synthesis problem. Additionally, to the best of the authors' knowledge, this remains an open problem in H_∞ control of uncertain systems in the literature. Existing methods typically provide only sufficient conditions for control design in such cases. Hence, as stated in Lemma 2, performance is guaranteed if there exist matrices that satisfy the LMI conditions; however, the existence of such matrices is not formally proven. Consequently, depending on the choice of certain variable values—such as β and the chosen limits for G and Z—the optimisation problem may fail to converge.

3.1 Control Co-design Framework. A bi-level co-design optimisation adopted in this paper involves two nested loops in which each overarching physical parameter is optimised, and during each iteration, the controller is also optimised, though constrained by the current value of the physical parameter. In other words, the outer loop optimises the plant values, while the inner loop focuses on optimising the controller for each plant configuration selected in the outer loop [31]. It can be described according to the equation below.

$$\min_{\mathrm{x_p}} \left\{ w_p \psi(\mathrm{x_p}) + w_c \int_{t_o}^{t_f} \Psi(\xi(t), \mathrm{x_{p*}}, \mathrm{x_c}, t)\, dt \right\},$$

$$\text{subject to: } g\left(x_p\right) \le 0, \quad (19)$$

$$\Gamma\left(t, \xi(t), x_{p*}, x_c\right) \le 0,$$

$$\varsigma\left(\xi(t_0), \xi(t_f), x_{p*}, x_c\right) \le 0,$$

where x_p and x_{p*} represent a candidate plant design and the optimal plant design, respectively; x_c denotes the control parameters, g are constraints dependent on the plant design, ψ is the plant design objective function, ξ represents the states, and $\{w_p, w_c\}$ are the objective weights.

ASME Letters in Dynamic Systems and Control. Received November 01, 2024;
Accepted manuscript posted May 8, 2025. doi:10.1115/1.4068615

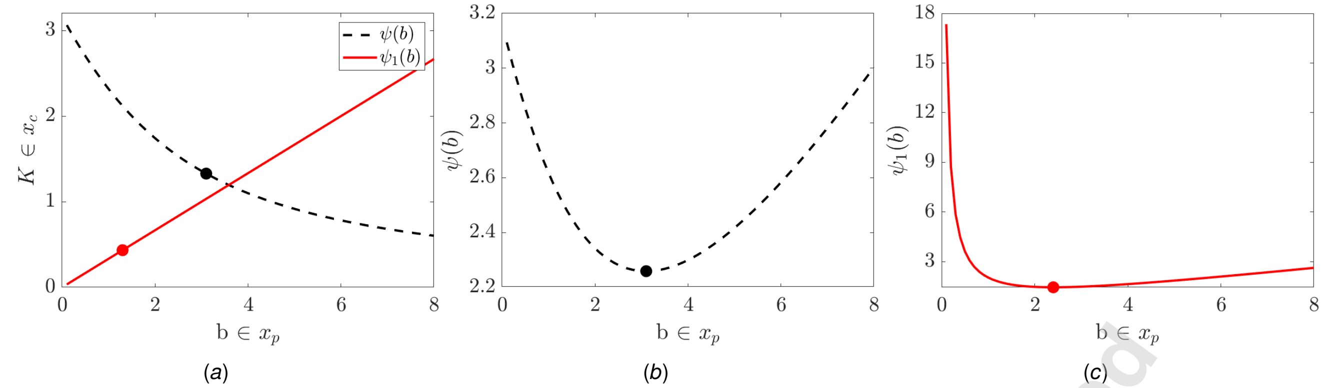

Fig. 3 Scalar plant problem results with $q = 10$, $r = 1$, $w_c = 1$, $\xi_0 = 1$, and $w_p = 0.3$: (a) Comparison of the controller cost, $\Psi(x_p, x_c)$, between two cost functions, $\psi(b)$ (dashed black) as expressed in Eq. (21), which follows the traditional LQR formulation, and $\psi_1(b)$ (solid red) as defined in Eq. (22) and adopted in this paper. (b) Cost function, $\psi(b)$, using LQR. (c) Cost function, $\psi_1(b)$, using H_∞ norm. *Source: elaborated by the authors.*

The objective is to minimise the cost function, which typically represents the total expected cost over a time horizon from t_0 to t_f, in which the controller cost $\Psi(\xi(t), \mathrm{x}_{p*}, \mathrm{x}_c, t)$ is the Lagrange term [45]. The path constraint $\Gamma(t, \xi, x_c, x_p) \leq 0$ ensures that the state and control variables meet certain conditions at all times. The boundary condition $\varsigma(\xi(t_0), \xi(t_f), x_{p*}, x_c) \leq 0$ ensures that the initial and final states of the system satisfy specified conditions, which could relate to state values or conservation laws. Here, we posit that this form of objective function serves as a unified criterion for both physical and control system design considerations.

Typically, the bi-level approach assumes the availability of a feasible controller design for each feasible system design, where traditional controllability constraints are presumed to ensure the viability of this model in linear systems, with LQR serving as the optimal control solution. This method has been widely adopted in CCD studies [17,29], where the optimal control gain is computed using the Riccati Equation, which for continuous systems can be expressed as:

$$A'S + AS - SBR^{-1}B'S + Q = 0,$$

$$K = R^{-1}B'S, \tag{20}$$

$$\Gamma := \mathrm{rank}\left(\begin{bmatrix} B & AB & \cdots & A^{n-1}B \end{bmatrix}\right) = n,$$

here, $A \in \mathbb{R}^{n\times n}$ and $B \in \mathbb{R}^{n\times n_u}$ are system matrices, $Q \in \mathbb{R}^{n\times n}$, $Q = Q' \geq 0$ and $R \in \mathbb{R}^{n_u\times n_u}$, $R = R' > 0$ are the weighting matrices that relates the significance of state and control efforts within the optimisation process respectively; and $S = S' \geq 0$ is the solution for Riccati Equation [46].

The alternative method proposed in this paper assumes that the optimisation problem, which minimises the system's H_∞ norm/guaranteed cost as described in Lemmas 1 and 2, can be integrated into the CCD formulation, instead of LQR formulations.

Figure 2 illustrates the bi-level CCD approach used in this work. The CCD problem is structured with an outer loop for plant design variables and an inner loop for control design variables. In the outer loop, plant constraints, $g(x_p)$ are initially applied to ensure physical feasibility. A plant candidate is then selected, and the H_∞ norm/guaranteed cost is calculated. Multiple plant design candidates are evaluated within the constrained physical domain until the plant that minimises the H_∞ norm/guaranteed cost is identified.

Once the optimal physical variables, x_p*, that minimise the H_∞ norm/guaranteed cost are found, these values are kept fixed, and the control variables are adjusted to determine the optimal control parameters. Here, both the H_∞ value and the slack variables Z, H, G, and β, as previously defined, or their constraints, Γ and ς, are considered as controller design variables, x_c. The objective is again to minimise the H_∞ norm/guaranteed cost for the system.

After settling the control variables to achieve the minimum control cost, the process is repeated. In this iteration, $x_{c,opt}$, the control variables that ensure the minimum control cost, are fixed, while the physical parameters are adjusted again to minimise the combined plant/controller cost function expressed in Eq. (19), and the final solution, $\{x_{c,opt}; x_{p,opt}\}$, is found.

4 Case Studies

To illustrate the method presented in the previous sections, this section revisits two previously addressed control co-design problems in the literature: a scalar plant and an active car suspension system.

The optimisation problems in Lemmas 1 and 2 were solved using SDP, which can be implemented using the YALMIP parser [22], ROLMIP parser [47], and solved via the SeDuMi solver [23]. The simulations were conducted using MATLAB version R2023a on a computer equipped with a 12-core CPU, CORE i9-10920XE, 64 GB of RAM, and a NVIDIA T400 4GB GPU, running Windows 11 Enterprise, version 22H2. The routines utilised for these simulations are available in [48].

4.1 Case Study 1: Scalar Plant. Consider the typical co-design formulation borrowed from the literature [17], which separates control and plant objectives, with no path constraints:

$$\begin{aligned} \min_{b,K} \quad & \psi(b) = \frac{w_c}{\xi_0^2}\int_0^\infty \left(q\xi^2 + ru^2\right)dt + w_p b \\ \text{subject to:} \quad & \dot{\xi} = -b\xi + u \\ & g_1 := \xi(0) - \xi_0 = 0 \\ & g_2 := -b \leq 0, \quad g_3 := -K \leq 0 \end{aligned} \tag{21}$$

where $u = -K\xi$, $b \in x_p$ (plant domain), $K \in x_c$ (controller domain), and ξ are the states. Although it is a simple scalar plant, this problem demonstrates important co-design concepts and has been addressed in early co-design formulations [31].

The modification adopted in this paper, expressed in the optimisation problem (22) is in terms of the new cost function, which accounts for the H_∞ norm instead of the traditional infinite time horizon optimisation of control gains. A precisely known system was considered for computing the H_∞ norm for each $b \in x_p$ and an optimisation problem was considered using the conditions presented in Lemma 1 for minimisation of the H_∞ norm. Additionally, the constraints are modified to suit the robust control problem. The aim is to achieve better-conditioned gains relative to the problem without these constraints.

$$\begin{aligned} \min_{b,\gamma} \quad & \psi_1(b) = \frac{w_c}{\xi_0^2}\gamma + w_p b \\ \text{subject to:} \quad & \dot{\xi} = -b\xi + u + w \\ & \Gamma_1 := 1 \leq Z \leq 3 \end{aligned} \tag{22}$$

where, γ, Z are the same as defined in inequalities (5) to (13), w is the disturbance term and $z(t) = \xi(t)$ is the output of the system.

Figure 3(a) illustrates the gains associated with a full-state feedback optimal LQR control law, together with the gain calculated using the method presented in Lemma (1), which can facilitate the development of potential inner-loop optimal control designs within the nested formulation for the two cost functions adopted: the black dashed line corresponds to the gains for the cost function in (21), the solid red line relates to the gains for the cost function in (22), and the solid dots represent the gains that guarantee the minimisation for each cost function. On the other hand, Figures 3(b) and 3(c) show the values for the cost functions $\psi(b)$ and $\psi_1(b)$, respectively. These results demonstrate that, by iterating through this particular set of values for the plant parameters, the gains for the LQR formulation and the formulation adopted in the present work assume different values.

ASME Letters in Dynamic Systems and Control. Received November 01, 2024;
Accepted manuscript posted May 8, 2025. doi:10.1115/1.4068615

Furthermore, it is generally recognised that LMI-based co-design methods do not always guarantee convergence to an optimal co-design solution [31]. While this issue is typically associated with iterative methods rather than nested ones, this example demonstrates that, despite the two cost functions being different, they exhibit similar behaviour.

Additionally, this example serves to illustrate that the proposed framework is not confined to systems with parametric uncertainties. A precisely known system can be seen as a special case in which the dimension of the polytope is one; therefore, the conditions presented in Lemma 2 can be applied equally to such a system. Consequently, using a simple scalar plant without uncertainties highlights the versatility of our approach and reaffirms that the methodology remains valid for systems with a fully specified model. Alternatively, the next example illustrates how the method is applied within the context of systems with polytopic uncertainties.

4.2 Case Study 2: Active Suspension. Figure 4 illustrates an active car suspension system characterised by the spring constant k_s and damping coefficient b per wheel. The tyre system is modelled as a spring-damping mechanism, defined by k_t and b_t, and mass m_1. On the other hand, m_2 represents one-quarter of the vehicle's total mass. The control objective is to minimise the vertical acceleration of the vehicle as it traverses uneven surfaces.

An actuator operates on the suspension system in accordance with a feedback state control law, $u = K\xi$, generating a force aimed at minimising the acceleration. Variations in road height, $w(t)$, relative to the road reference level, are incorporated into these formulations as disturbances. Lastly, $h_2(t)$ and $h_1(t)$ represent the heights of the vehicle body and wheel, respectively. This problem exemplifies a typical real-world control challenge in the automotive industry, and a similar problem has been studied within the framework of co-design [18,29] and robust control [21].

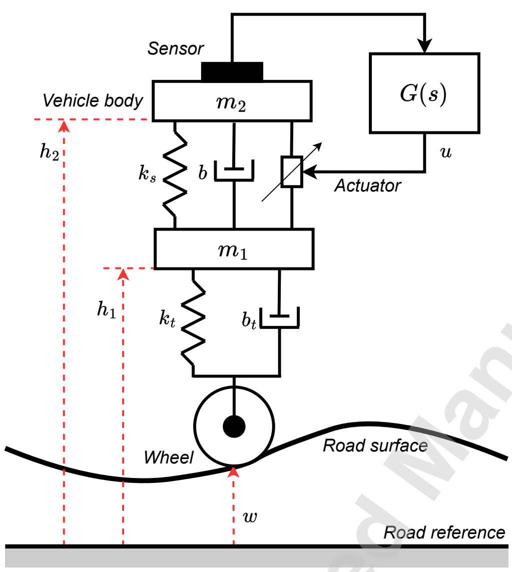

Fig. 4 A schematic of the active vehicle suspension system. *Source: elaborated by the authors, adapted from [21].*

4.2.1 Control Oriented Model. The Euler-Lagrange formulation considers the kinetic energy, and elastic potential energy, described by Eqs. (23) and (24), respectively, to derive the equations of motion [21].

$$E_k = \frac{1}{2}m_2\dot{h}_2^2 + \frac{1}{2}m_1\dot{h}_1^2, \tag{23}$$

$$E_p = \frac{1}{2}k_s(h_2 - h_1)^2 + \frac{1}{2}k_t h_1^2, \tag{24}$$

A dissipation function, denoted as F_d, can be defined to account for the energy loss caused by dissipative forces, such as damping

$$F_d = \frac{1}{2}b(\dot{h}_2 - \dot{h}_1)^2, \tag{25}$$

The modified Euler-Lagrange equations including dissipation are described as follows:

$$\begin{gathered}\frac{d}{dt}\left(\frac{\partial L}{\partial \dot{q}_i}\right) - \frac{\partial L}{\partial q_i} + \frac{\partial F_d}{\partial \dot{q}_i} = Q_i,\\ L = E_k - E_p,\\ i = 1, 2, \ldots, n,\end{gathered} \tag{26}$$

where Q_i are the generalised forces applied. The generalised coordinates of the system are the height of the vehicle chassis, $h_2(t)$, and the height of the tire system, $h_1(t)$. The forces acting on the system include the control input, $u(t)$, applied by the active damper between the masses m_1 and m_2, and the wheel height variation, $w(t)$, which is considered as the force acting on the wheel.

A state-space representation is obtained for the system:

$$\begin{gathered}\dot{\xi} = \begin{bmatrix} -\frac{b}{m_2} & \frac{b}{m_2} & -\frac{k_s}{m_2} & \frac{k_s}{m_2} \\ \frac{b}{m_1} & -\frac{b}{m_1} & \frac{k_s}{m_1} & -\frac{k_s+k_t}{m_1} \\ 1 & 0 & 0 & 0 \\ 0 & 1 & 0 & 0 \end{bmatrix} \begin{bmatrix}\xi_1\\ \xi_2\\ \xi_3\\ \xi_4\end{bmatrix} + \begin{bmatrix}\frac{1}{m_2}\\ \frac{-1}{m_1}\\ 0\\ 0\end{bmatrix} u + \begin{bmatrix}0\\ \frac{1}{m_1}\\ 0\\ 0\end{bmatrix} w,\\ z = \begin{bmatrix} 0 & 0 & 1 & 0 \\ 0 & 0 & 0 & 1 \end{bmatrix} \begin{bmatrix}\xi_1\\ \xi_2\\ \xi_3\\ \xi_4\end{bmatrix}, \text{ where } \xi = \begin{bmatrix}\xi_1\\ \xi_2\\ \xi_3\\ \xi_4\end{bmatrix} = \begin{bmatrix}\dot{h}_2\\ \dot{h}_1\\ h_2\\ h_1\end{bmatrix},\\ D_{zu} = 0, \quad D_{zw} = 0.\end{gathered} \tag{27}$$

4.2.2 Physical Design. The physical design adopted here is derived from Ref. [18]. The stiffness formula is given by

$$k_s = \frac{d^4 G}{8D^3 N_a\left(1 + \frac{1}{2C^2}\right)}, \tag{28}$$

where, d is the wire diameter, D is the helix diameter, and p is the spring pitch, N_a is the number of active coils, the shear modulus is $G = 77.2\ GPa$, and the spring index, $C = D/d$, is related to how easily a spring can tangle. A schematic of the spring system can be seen in Fig. 5(*a*).

On the other hand, the formula to calculate the suspension damper coefficient is given by:

$$\mathrm{b} = \frac{D_p^4}{8C_d C_2 D_0^2}\sqrt{\frac{\pi k_v \rho_1}{2}}, \tag{29}$$

where, D_0 and D_p, are the valve diameter and the working piston diameter, respectively; $C_d \approx 0.7$ is the discharge coefficient, $k_v = 7500\ N/m$ is the spool valve spring constant, $\rho_1 = 850\ kg/m^3$ is the damper fluid density, and $C_2 = \eta A_f\sqrt{x_m}$ is the damper valve coefficient, in which $A_f = 0.1$ is used to tune the port shape, $x_m = \frac{A_0 P_{allow}}{k_v}$ is the maximum valve lift (x_v) at the maximum allowed damper pressure, $P_{allow} = 4.75 \times 10^6\ Pa$, and $A_0 = \frac{\pi D_0^2}{4}\ m^2$ is the spool valve frontal area. A schematic of the damper system can be seen in Fig. 5(*b*).

The physical constraints for plant design were selected based on several aspects, such as interference with other vehicle components, permanent spring deformation, spring buckling, linearity of damper behaviour, maximum damper pressure, and thermal considerations, among others. All of these considerations have been omitted in this paper but are detailed in the aforementioned literature [18]. Based on these physical considerations, the plant design vector, $x_p = [d, D, p, Na, D_0, D_p, D_s]$, was established as described below.

$$x_{p,min} = [0.005, 0.05, 0.02, 3, 0.003, 0.03, 0.1],$$

$$x_{p,max} = [0.02, 0.4, 0.5, 16, 0.012, 0.08, 0.3].$$

By replacing these values of the plant design vector in Eq. (28) and (29), the minimum and maximum suspension stiffness constant and damper values were derived, as shown in Table 1.

4.2.3 Control Design. Let $x_c = \{x_{c1}, x_{c2}, x_{c3}, x_{c4}\}$ be the control design variable. Then, x_{c1} is defined such that:

$$\begin{gathered} x_{c1} := range_i = \sigma_i^{\max} - \sigma_i^{\min}, \quad range_i \in \mathbb{R} \\ [\sigma_i^{\min}, \sigma_i^{\max}] \subseteq [x_{p,min}; x_{p,max}], \quad i = 1, 2, \ldots, N, \end{gathered} \tag{30}$$

ASME Letters in Dynamic Systems and Control. Received November 01, 2024;
Accepted manuscript posted May 8, 2025. doi:10.1115/1.4068615

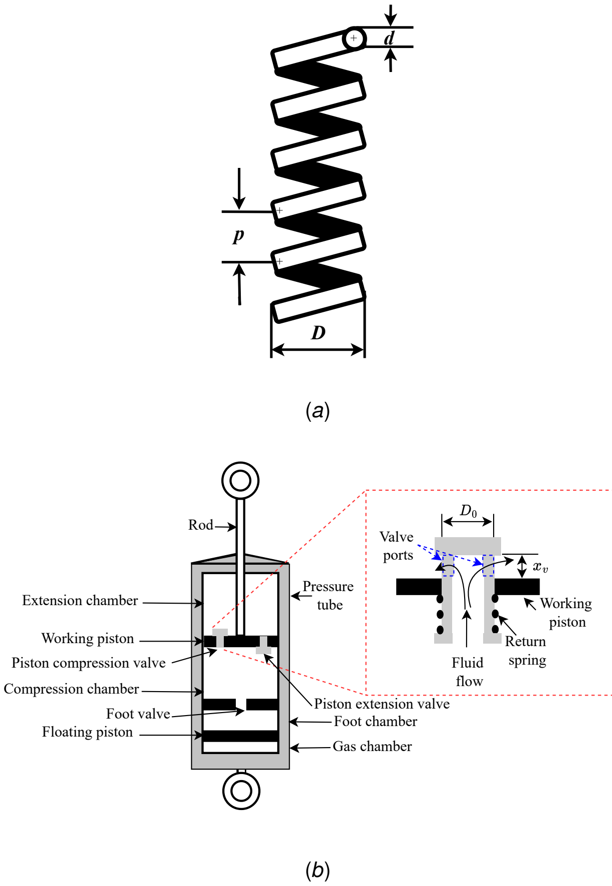

Fig. 5 (*a*) Schematic of a helical compressing spring. (*b*) A telescopic damper with a piston compression valve. *Source: elaborated by the authors, adapted from [18].*

with $range_i$ modelling the size of the uncertainty in a parameter, and σ_i defined as any uncertain physical parameter, such that $\sigma_i^{\min} \le \sigma_i \le \sigma_i^{\max}$. Hence, $\sigma_i(\alpha) = \alpha_k \sigma_i^{\min} + \alpha_q \sigma_i^{\max}$ represents all possible values of $\sigma_i \in [\sigma_i^{\min}, \sigma_i^{\max}]$, with $\{\alpha_k, \alpha_q\} \in \Lambda_N$, $\{k, q\} = 1, 2, \ldots, N$, and Λ_N defined in Eq. (3). Then, the system in Eq. (27) can be represented as an uncertain system, as shown in Eq. (1).

To evaluate the combination of control co-design structure with systems modelled with parametric uncertainties, m_1, m_2, k_t, and b_t were considered to be precisely known, with values indicated in Table 1, while b and k_s were considered to be the uncertain parameters. For simplicity, a single range of uncertainty was considered for each of the uncertain parameters, also described in the Table 1.

The Algorithm 1 describes the second control design variable, x_{c2}, which is related to defining the values of b and k_s that minimise the H_∞ guaranteed cost. An iterative process is established until the optimal candidates, b_* and $k_{s,*}$, are determined.

However, minimising the guaranteed cost alone may not suffice, as the actual implementation depends on a physical actuator, which has limitations in terms of the maximum control force it can exert and is part of a system with finite energy. For instance, the control force between the sprung and unsprung masses could be exerted by a linear motor. Similarly to the physical domain of the plant, where restrictions were necessary—though not detailed in this work—due to the plant's physical viability, restrictions are also required in the control variable domain. This relates to the acceptable values for the maximum control force, which are dependent on the gain values.

To illustrate this, Figs. 6(*a*) and 6(*c*) show the effect of simultaneously varying the values of k_s and b on the H_∞ guaranteed cost and the norm of the gain K, respectively, when $\beta = \beta_{\text{initial}}$, $0 \le Z_{ij} \le 3$, and $G \ge \mathbf{0}_{4\times4}$. It can be observed that some regions with acceptable values for the H_∞ guaranteed cost correspond to areas with higher gains. Although in this example, all values of the H_∞ guaranteed cost fall within acceptable limits, better conditioning of the gain may be necessary to ensure compliance with

Algorithm 1: Optimisation of x_p (plant parameters)

Let $x_{c2} := \gamma$, γ defined in Lemma 2 ▹ Initialise γ (H_∞ guaranteed cost)
for $i = 1 : 1 : q$ **do** ▹ Iterate over all possible $b(i)$ values
  for $j = 1 : 1 : q$ **do** ▹ Iterate over all possible $k_s(j)$ values
    $\gamma(i, j) = \gamma(b(i), k_s(j), \beta_{initial})$, $b(i)$ and $k_s(j) \in x_p$ ▹ Compute γ for the given parameters
    if $\gamma < \gamma_{min}$ **then** ▹ Check if the new γ is the lowest found
      $b_* \leftarrow b(i)$ and $k_{s,*} \leftarrow k_s(j)$ ▹ Update optimal values
    end if
  end for
end for

actuator constraints.

Rather than detailing the specifics of the actuator, this work assumes that an arbitrary control force u can be achieved within the maximum force limits, constrained by physical feasibility. Consequently, a strategy for gain limitation has been adopted, treating the slack variables β, Z, and G, as defined in Lemma 2, as control design variables.

Following the identification of x_{c2}, the limits for the slack variables Z and G, as defined in Lemma 2, are established. The maximum and minimum bounds for these variables are determined to provide a feasible range for subsequent optimisation. Since the gain is expressed as $K = ZG^{-1}$, constraining these variables will inherently limit the gain. Therefore, the optimal set x_{c3} is defined as the argument that minimises the norm of K, and was chosen such that $0 \le Z_{ij} \le 3$, $\forall\ i, j$, and $G = G' \ge \mathbf{I}$.

With the optimal candidates b_* and $k_{s,*}$ identified, the next step is, therefore, to determine the optimal value of β, as shown in Algorithm 2. The values for β follow a logarithmic progression, spanning $\beta \in [10^{-9}, 10^3]$. The choice of this range was made based on the values of β for which the optimisation problem converges. The algorithm tracks the smallest 2-norm of gain K encountered and updates β_{opt} whenever a new minimum is found. This step ensures that β_{opt} is the value of β that minimises the gain K.

Algorithm 2: Optimisation of β parameter

Let $x_{c4} := \beta$, with β defined in Lemma 2. ▹ Initialise β (scalar LMI variable)
for $i = 1 : 1 : m$ **do** ▹ Iterate over all possible $\beta(i)$ values
  $\|K\| := K(b_*, k_{s,*}, \beta(i))$ ▹ Compute $\|K\|$ (the norm of the gain K) using current $\beta(i)$
  if $\|K\| < \|K\|_{min}$ **then** ▹ Check if the new $\|K\|$ is the lowest found
    $\beta_{opt} \leftarrow \beta(i)$ ▹ Update optimal β value
  end if
end for

Figures 6(*b*) and 6(*d*) show the effect of assuming the values $\beta = \beta_{opt}$, $0 \le Z_{ij} \le 3$, and $G = G' \ge \mathbf{I}$ on the H_∞ guaranteed cost and the magnitude of the feedback gain, respectively. A new region of optimality is observed, with the values for the H_∞ being slightly higher compared to the previous case. However, the gain values are now lower, on the order of 10^9. This not only demonstrates the preservation of the H_∞ guaranteed cost but also ensures that the gains remain within the limits of physical feasibility.

SeDuMi primarily employs a self-dual embedding interior-point method based on self-concordance to solve convex conic problems. Consequently, we do not have direct control over the smoothness of the controller gain norms presented in Fig. 6(*c*) and 6(*d*). The solver returns any feasible gain values that satisfy the optimisation constraints, and thus, variations in smoothness may naturally arise due to the numerical optimisation process. Additionally, we explored the influence of adding restrictions to the decision variables (slack LMI variables Z and G), which could theoretically affect the smoothness of the results. Interestingly, we observed that imposing these restrictions to ensure a feasible gain region actually led to a reduction in non-smoothness rather than exacerbating it.

Finally, a combined plant/controller optimisation objective, J, is defined. With $x_{c3,\text{opt}}$ and $x_{c4,\text{opt}}$ held constant, the algorithm iterates through the

ASME Letters in Dynamic Systems and Control. Received November 01, 2024;
Accepted manuscript posted May 8, 2025. doi:10.1115/1.4068615

Table 1 Values for physical and control parameters

Parameter	Value [SI]	Parameter	Value [SI]
m_1	65	$range_1$	15
m_2	325	$range_2$	15
k_t	232.5×10^3	$\beta_{initial}$	1×10^{-1}
b_t	0	$k_{s,*}$	$\in [1.6003 \times 10^4, 1.6018 \times 10^4]$
k_s	$\in [1.5059 \times 10^3, 1.6018 \times 10^4]$	b_*	$\in [8.4456 \times 10^3, 8.4606 \times 10^3]$
b	$\in [6.6731 \times 10^3, 8.4606 \times 10^3]$	$x_{c3,opt}$	$0 \leq Z_{ij} \leq 3, G = G' \geq \mathbf{I}$
G	77.2×10^9	β_{opt}	1×10^{-4}
A_f	0.1		
C_d	0.7		
k_v	7500		
ρ_1	850		
P_{allow}	4.75×10^6		

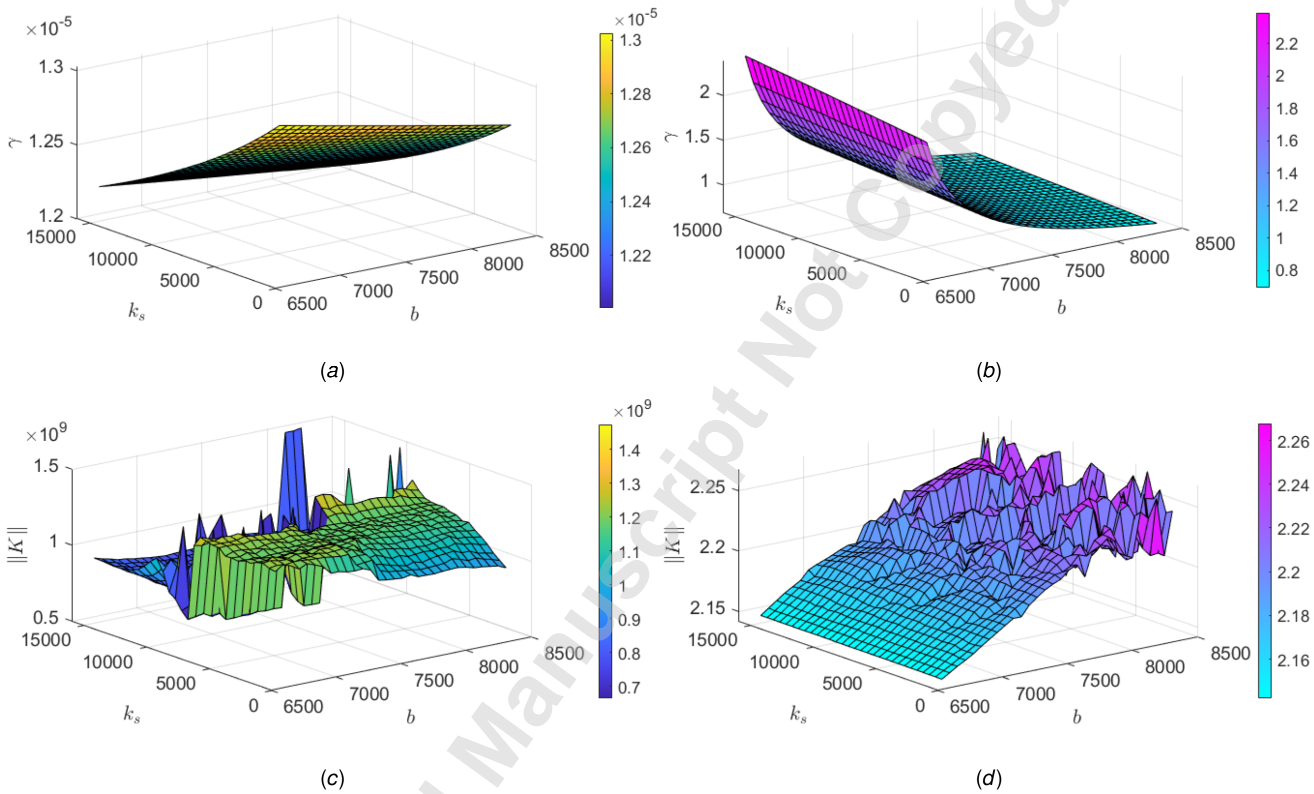

Fig. 6 Effect of simultaneously varying the values of stiffness and damping on the H_∞ guaranteed cost, and on the norm of the gain, $\|K\|$. *(a)(c)* The value for β was assumed to be $\beta_{\text{initial}} = 1 \times 10^{-1}$, with $0 \leq Z_{ij} \leq 3$ and $G \geq 0_{4x4}$. *(b)(d)* The effect of altering the values of x_{c3} and x_{c4} was evaluated with $\beta_{opt} = 1 \times 10^{-4}$, $0 \leq Z_{ij} \leq 3$, and $G = G' \geq \mathbf{I}$. *Source: elaborated by the authors.*

previously defined ranges of b and k_s using a set of nested loops. For each combination of b and k_s, the H_∞ guaranteed cost is recalculated, and the cost function is assessed. The function J integrates parameters and functions such as $\lambda(t)$, $\ddot{h}_2(t)$, and $u(t)$, which represent handling, comfort, and control cost, respectively. The algorithm updates b_{opt} and $k_{s,\text{opt}}$ to the values that minimise J, ensuring an optimal design configuration, as shown in Algorithm 3.

The cost function used in this case study is an adaptation of some presented in the literature [18,29] and is described below:

$$J = \int_0^{t_F} \left(r_1 \lambda^2 + r_2 \ddot{h}_2^2 + r_3 u^2 \right) dt + r_4 \gamma, \quad (31)$$

with $\lambda = (h_1 - w)$, $r_1 = 10^3$, $r_2 = 5$, $r_3 = 1$, and $r_4 = 10^1$. The adaptation involves the addition of the term $r_4\gamma$ to account for the H_∞ guaranteed cost of the system. Additionally, the weights r_1, r_2, r_3, and r_4 ensure

Algorithm 3: Optimisation of J cost function

```
for i = 1 : 1 : p do                 ▷ Iterate over all possible b(i) values
    for j = 1 : 1 : p do             ▷ Iterate over all possible k_s(j) values
        γ(i, j) = γ(b(i), k_s(j))    ▷ Compute γ based on parameters
        J(i, j) = J(γ(i, j), u(t), ḧ_2(t), λ(t)), J defined in Eq. (31)
                                     ▷ Evaluate the cost function J
    end for
end for
[b_opt, k_s,opt] ∈ x_p := arg min_{x_p} J   ▷ Find optimal parameters by minimising J
```

ASME Letters in Dynamic Systems and Control. Received November 01, 2024;
Accepted manuscript posted May 8, 2025. doi:10.1115/1.4068615

approximately the same magnitude for each component of the objective function.

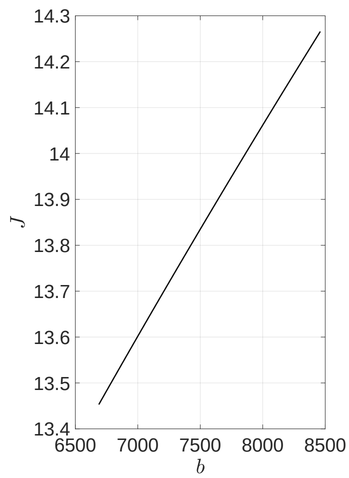

(*a*)

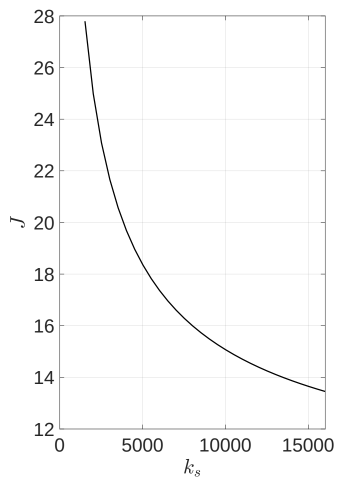

(*b*)

Fig. 7 (*a*) Effect of varying the values of damping with fixed stiffness, $k_{s,opt}$, on the cost function J, as defined in Eq. (31), for the rough road. (*b*) Effect of varying the values of stiffness with fixed damping, b_{opt}, on the cost function J, as defined in Eq. (31), for rough road. *Source: elaborated by the authors.*

One can see in Fig. 7 the individual effect of each of the uncertain parameters on the computation of the cost function expressed in Eq. (31) when the other parameter is set to its optimal value for a rough road. Considering the lowest cost, J, the optimal parameters were established, as expressed in Table 2. Observe that, since the parameters are uncertain, they belong to the interval $[\sigma_i^{\min}, \sigma_i^{\max}]$, as defined in Eq. (30) and Table 1.

Table 2 Solution for the plant/controller optimisation problem

Parameter	Value
$k_{s,opt}$	$\in [1.6003 \times 10^4, 1.6018 \times 10^4]$
b_{opt}	$\in [6.6731 \times 10^3, 6.6881 \times 10^3]$

Figures 8(*a*) through 8(*c*) illustrate the disturbance modelled as variations in a rough road surface and the dynamic response of the system. The results show that the approach adopted in this work is effective in minimising the vehicle's vertical acceleration. Specifically, the solution to this CCD problem requires setting the stiffness rate to the maximum value within the interval considered for x_p, while the damping rate should take the opposite approach.

This choice arises from how the plant and control variables were selected, such as in the cases of x_{c3} and x_{c4}, which were chosen to minimise control gain. This approach suggests a preference for prioritising the passive dynamics of components when designing the suspension, rather than relying on brute control force. However, more than just optimising passive dynamics, the CCD framework enables a combined plant/controller optimisation. This is critical, as suspension performance depends on whether it is an active or passive system. In other words, optimising passive dynamics alone may be insufficient depending on the desired performance and external inputs. For instance, in real scenarios where the vehicle encounters rough, uneven surfaces, a passive suspension might not provide the expected comfort for passengers, highlighting the need for active suspension systems like the one proposed in this paper. Nonetheless, passive and active components can sometimes compete rather than complement each other, a well-recognised issue in suspension systems [29]. This coupling between plant and controller optimisation underscores the value of co-design, as demonstrated by this example.

For comparison, Fig. 8(*c*) illustrates the system's response when the plant parameters were set to the optimal values identified in this study, and two control strategies were applied: the method proposed in this paper and the traditional LQR formulation, with weighting matrices $Q = C_z C_z'$ and $R = 10$. Although the performance difference between the two controllers is small, the approach introduced in this paper demonstrates superior performance, exhibiting lower overshoot and improved settling time. Additionally, it offers greater versatility compared to LQR, particularly in terms of incorporating decision variables for CCD design and integrating control optimisation sub-problems.

The methodology presented in this work successfully achieves the objective of connecting CCD frameworks with systems that incorporate parametric uncertainties and are subject to disturbances. Regarding the acclaimed optimality in co-design applications, H_∞ control plays a critical role in minimising the impact of exogenous inputs on system performance. The LMI conditions proposed in this paper not only provide sufficient conditions to ensure a bound on the guaranteed cost for H_∞ control, but also offer a straightforward means of expressing stability and synthesis conditions, allowing for flexibility in control system design. In addition, unlike classical optimal control methods, where the trade-off between performance metrics and control expenditure is managed through two Hermitian positive-definite matrices—adding conservatism to the design by limiting control flexibility—this approach allows for greater freedom in selecting plant and controller parameters. These parameters can be treated as independent design variables in co-design problems, facilitating a less conservative and more adaptable design framework. In this case study, for example, we only considered k_s and b as uncertain parameters. However, uncertainty could be introduced into any plant parameter, though this would increase the dimension of the polytope.

We limited our approach to introducing new slack variables into the LMI control design conditions to reduce the conservatism of the method proposed in Lemma 1. Other strategies could involve the use of parameter-dependent matrices and the consideration of decision variables as homogeneous polynomially parameter-dependent variables of any chosen degree. These techniques have been widely applied in polytopic systems [34,35] and can be incorporated by making simple adjustments to the LMI conditions in Section 3. With this approach, additional control design variables could be included. For example, we limited gain by constraining the slack variables Z and G; however, constraints on the plant, control, and state could also be directly incorporated into the LMI conditions. This flexibility highlights the adaptability of the method presented in this paper.

CCD inherently involves the simultaneous optimisation of plant and control parameters, often requiring iterative procedures over a range of values and typically implementing modifications in a parametric manner. Additionally, all physical modelling inherently contains approximations and uncertainties. These approximations and uncertainties, when combined with CCD, become even more critical, as the interdependency between plant and control increases the complexity of the design space and amplifies the impact of uncertainties. Therefore, these issues could be exacerbated, making techniques that address uncertainties and unknown dynamics, such as robust control, even more essential. Hence, the methodology presented in this work provides a powerful means to handle these challenges effectively.

Additionally, a key advantage of using parametric uncertainties, as done in this work, is the computational efficiency it can bring to CCD approaches.

ASME Letters in Dynamic Systems and Control. Received November 01, 2024;
Accepted manuscript posted May 8, 2025. doi:10.1115/1.4068615

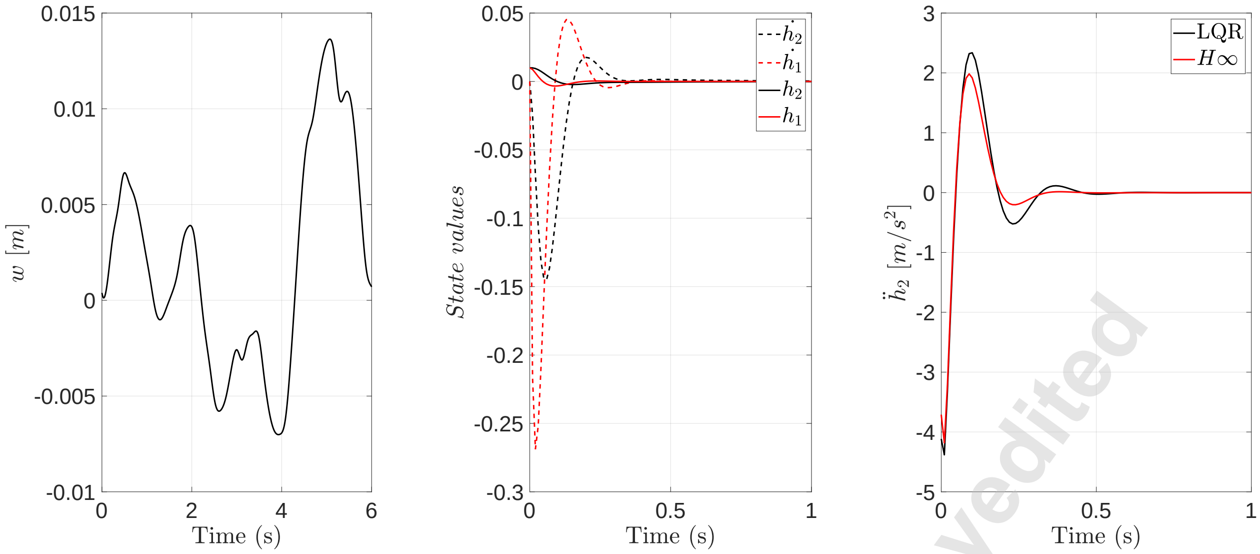

(a) (b) (c)

Fig. 8 ***(a)*** **Road surface, $w(t)$, modelled as a rough road.** ***(b)*** **The system response for optimal parameter values obtained through the bi-nested CCD approach, combined with a feedback gain that minimises the H_∞ guaranteed cost, as adopted in this work, is considered for the case where $\alpha_1 = \cdots = \alpha_n$. State values: vehicle body and wheel positions, along with vertical velocities, are measured outputs for rough road input.** ***(c)*** **Vehicle vertical acceleration, using H_∞ as adopted in this work (red line), for the case where $\alpha_1 = \cdots = \alpha_n$, and the traditional LQR (black line) with weight matrices $Q = C_z C_z'$ and $R = 10$.** ***Source: elaborated by the authors.***

CCD often requires evaluating a large number of candidate solutions across a given range of plant parameters, which can be computationally expensive. Although no computational metrics were presented in the current paper, our approach suggests a more structured way of handling this, as it offers a method to break the original CCD parameter candidate range into smaller subintervals. These subintervals could be treated as uncertain candidates, and the search for an optimal candidate could then be performed. In a second step, once an optimal parameter region is identified, a refined search within this narrowed range can be conducted, now considering the parameters within this reduced interval as known. By reducing the total number of candidates that need to be explicitly evaluated, this method can significantly decrease computational effort while still preserving robustness. However, this will be addressed in future work.

The method presented in this paper is especially beneficial for applications where disturbance rejection and robustness are critical, such as in active suspension systems, autonomous systems, and energy systems exposed to varying environmental conditions. However, while the H_∞ control minimises the worst-case impact of disturbances, it does not necessarily yield the best performance in terms of steady-state tracking or transient response when disturbances are small.

5 Conclusion

This study has made significant progress in bridging the gap between control co-design and robust control by extending CCD to systems with exogenous inputs and parametric uncertainties. The proposed methodology, which employs H_∞ control to minimise the influence of disturbances and ensure system stability, has been validated through numerical examples involving a scalar plant and an active car suspension system. The results indicate that the integration of CCD with robust control strategies not only guarantees system performance but also provides a systematic approach for managing uncertainties within a polytopic framework.

Comparing different control co-design formulations using the framework adopted in this paper and evaluating the computational cost associated with each approach is left for future work. Given that the CCD framework has been recently applied in the context of wave energy converters and floating offshore wind platforms [6,7,49,50], a future study could focus on these systems, considering the challenge of predicting ocean wave conditions. This could involve applying the current framework while accounting for unforeseen wave frequencies as disturbances. Lastly, a similar framework to the one presented in this paper could consider the adoption of either the optimal H_∞ norm/guaranteed cost, H_2 norm/guaranteed cost, or a mixed H_∞ and H_2 approach as the controller, instead of solely using the H_∞ norm/guaranteed cost.

Funding Data

- This publication has emanated from research conducted with the financial support of Taighde Éireann – Research Ireland under Grant number 21/FFP-P/10065. Erivelton Nepomuceno was supported by Brazilian Research Agency CNPq (Grant No. 444154/2024-8).

Nomenclature

α = Uncertainty parametrisation element
$\Xi_i, \Xi(\alpha)$ = The i-th vertex of a polytopic domain, and the representation of any uncertain matrix, respectively
Λ_N = A unit simplex set of dimension N
w_p, w_c = Weights on plant and controller objectives
u = Control input
ψ = Plant design objective function
Ψ = Controller cost function
Γ, ς = Controller constraints
P = Lyapunov matrix
Z, G, H = Matrix LMI slack variables
β = Scalar LMI variable
γ = H_∞ norm/guaranteed cost
μ = The square of the H_∞ norm/guaranteed cost
$\star$ = The transpose of a symmetric matrix block
$\mathbf{I}$ = Identity matrix
x_p = plant design variables
x_c = control design variables

Superscripts and Subscripts

z = related to the controlled output
u = related to the control input
w = related to the disturbance input
zu = related to the effect of control input in the controlled output
zw = related to the effect of disturbance input in the controlled output

$*, opt$ = Suboptimal and optimal, respectively
$'$ = The transpose of a matrix

References

[1] Allison, J. T., 2013, "Plant-Limited Co-Design of an Energy-Efficient Counterbalanced Robotic Manipulator," Journal of Mechanical Design, **135**(10), p. 101003, _eprint: https://asmedigitalcollection.asme.org/mechanicaldesign/article-pdf/135/10/101003/6222451/md_135_10_101003.pdf.

[2] Garcia-Sanz, M., 2019, "Control Co-Design: An engineering game changer," Advanced Control for Applications, **1**(1), p. e18, e18 ADC2-19-0039.

[3] Allison, J. T. and Herber, D. R., 2014, "Special Section on Multidisciplinary Design Optimization: Multidisciplinary Design Optimization of Dynamic Engineering Systems," AIAA Journal, **52**(4), pp. 691–710.

[4] Annaswamy, A. M., Johansson, K. H., and Pappas, G., 2024, "Control for societal-scale challenges: Road map 2030," IEEE Control Systems Magazine, **44**(3), pp. 30–32.

[5] Silva, J. G. d., Nazaré, T., Costa, M., Lacerda, M. J., and Nepomuceno, E., 2024, "Engineering and Technology Applications of Control Co-Design: A Survey," IEEE Access, **12**, pp. 81692–81717.

[6] Pao, L. Y., Pusch, M., and Zalkind, D. S., 2024, "Control Co-Design of Wind Turbines," Annual Review of Control, Robotics, and Autonomous Systems, **7**(1).

[7] Abbas, N. J., Jasa, J., Zalkind, D. S., Wright, A., and Pao, L., 2024, "Control co-design of a floating offshore wind turbine," Applied Energy, **353**, p. 122036.

[8] Coe, R. G., Bacelli, G., Olson, S., Neary, V. S., and Topper, M. B., 2020, "Initial conceptual demonstration of control co-design for WEC optimization," Journal of Ocean Engineering and Marine Energy, **6**(4), pp. 441–449.

[9] Peña-Sanchez, Y., García-Violini, D., and Ringwood, J. V., 2022, "Control co-design of power take-off parameters for wave energy systems," IFAC-PapersOnLine, **55**(27), pp. 311–316, 9th IFAC Symposium on Mechatronic Systems MECHATRONICS 2022.

[10] Naik, K., Beknalkar, S., Mazzoleni, A., and Vermillion, C., 2021, "Fused Geometric, Structural, and Control Co-Design Framework for an Energy-Harvesting Ocean Kite," *2021 American Control Conference (ACC)*, pp. 3525–3531, doi: 10.23919/ACC50511.2021.9483434.

[11] (NREL), N. R. E. L., 2023, "Wind Energy with Integrated Servo-control (WEIS)," Accessed: 2024-08-16, https://github.com/WISDEM/WEIS

[12] Zardini, G., Lanzetti, N., Salazar, M., Censi, A., Frazzoli, E., and Pavone, M., 2020, "On the Co-Design of AV-Enabled Mobility Systems," *2020 IEEE 23rd International Conference on Intelligent Transportation Systems (ITSC)*, IEEE, doi: 10.1109/itsc45102.2020.9294499.

[13] Khandekar, A. A., Siefert, J., and Li, P. Y., 2021, "Co-Design of a Fully Electric Hybrid Hydraulic-Electric Architecture (FE-HHEA) for Off-Road Mobile Machines," *2021 American Control Conference (ACC)*, pp. 352–357, doi: 10.23919/ACC50511.2021.9482615.

[14] Nakka, S. K. S. and Alexander-Ramos, M. J., 2021, "Simultaneous Combined Optimal Design and Control Formulation for Aircraft Hybrid-Electric Propulsion Systems," Journal of Aircraft, **58**(1), pp. 53–62.

[15] Zardini, G., Censi, A., and Frazzoli, E., 2021, "Co-Design of Autonomous Systems: From Hardware Selection to Control Synthesis," *2021 European Control Conference (ECC)*, IEEE, doi: 10.23919/ecc54610.2021.9654960.

[16] Zhu, Q. and Sangiovanni-Vincentelli, A., 2018, "Codesign Methodologies and Tools for Cyber–Physical Systems," Proceedings of the IEEE, **106**(9), pp. 1484–1500.

[17] Herber, D. R. and Allison, J. T., 2018, "Nested and Simultaneous Solution Strategies for General Combined Plant and Control Design Problems," Journal of Mechanical Design, **141**(1), p. 011402, _eprint: https://asmedigitalcollection.asme.org/mechanicaldesign/article-pdf/141/1/011402/6233143/md_141_01_011402.pdf.

[18] Allison, J. T., Guo, T., and Han, Z., 2014, "Co-design of an active suspension using simultaneous dynamic optimization," Journal of Mechanical Design, **136**(8), p. 081003.

[19] 2009, *On Measures of Coupling Between the Artifact and Controller Optimal Design Problems*, Vol. Volume 2: 29th Computers and Information in Engineering Conference, Parts A and B of International Design Engineering Technical Conferences and Computers and Information in Engineering Conference.

[20] Allison, J. T., 2014, "Engineering system co-design with limited plant redesign," Engineering Optimization, **46**(2), pp. 200–217.

[21] Garcia-Sanz, M., 2017, *Robust control engineering: practical QFT solutions*, CRC press.

[22] Löfberg, J., 2004, "YALMIP : A Toolbox for Modeling and Optimization in MATLAB," *In Proceedings of the CACSD Conference*, Taipei, Taiwan, doi: 10.1109/CACSD.2004.1393890.

[23] Sturm, J. F., 1999, "Using SeDuMi 1.02, A MATLAB toolbox for optimization over symmetric cones," Optimization Methods and Software, **11**(1-4), pp. 625–653.

[24] Geromel, J. and De Oliveira, M., 2001, "H/sub 2/ and H/sub /spl infin// robust filtering for convex bounded uncertain systems," IEEE Transactions on Automatic Control, **46**(1), pp. 100–107.

[25] Agulhari, C. M., Neto, J. M. M., Lacerda, M. J., de Souza, R. P. P., Castoldi, M. F., and Goedtel, A., 2021, "Robust real-time parameter estimation for linear systems affected by external noises and uncertainties," International Journal of Adaptive Control and Signal Processing, **35**(2), pp. 203–220.

[26] Oliveira, R. C. and Peres, P. L., 2005, "Stability of polytopes of matrices via affine parameter-dependent Lyapunov functions: Asymptotically exact LMI conditions," Linear Algebra and its Applications, **405**, pp. 209–228.

[27] Lacerda, M. J., Oliveira, R. C., and Peres, P. L., 2011, "Robust H2 and $H\infty$ filter design for uncertain linear systems via LMIs and polynomial matrices," Signal Processing, **91**(5), pp. 1115–1122.

[28] Moreira, J. F. D., da Silva, J. G., Peixoto, M. L., Nepornuceno, E., and Lacerda, M. J., 2024, "Event-Based Control for Discrete-Time Linear Parameter-Varying Systems: An Emulation-Based Design," *2024 UKACC 14th International Conference on Control (CONTROL)*, pp. 49–54, doi: 10.1109/CONTROL60310.2024.10532022.

[29] Fathy, H., Papalambros, P., Ulsoy, A., and Hrovat, D., 2003, "Nested plant/controller optimization with application to combined passive/active automotive suspensions," *Proceedings of the 2003 American Control Conference, 2003.*, Vol. 4, pp. 3375–3380 vol.4, doi: 10.1109/ACC.2003.1244053.

[30] Allison, J. T. and Nazari, S., "Combined Plant and Controller Design Using Decomposition-Based Design Optimization and the Minimum Principle," *Proceedings of the ASME 2010 International Design Engineering Technical Conferences and Computers and Information in Engineering Conference*, Vol. 1, ASME, Montreal, Quebec, Canada, pp. 765–774, doi: 10.1115/DETC2010-28887.

[31] Fathy, H., Reyer, J., Papalambros, P., and Ulsov, A., 2001, "On the coupling between the plant and controller optimization problems," *Proceedings of the 2001 American Control Conference. (Cat. No.01CH37148)*, Vol. 3, pp. 1864–1869 vol.3, doi: 10.1109/ACC.2001.946008.

[32] Papalambros, P. Y. and Wilde, D. J., 2000, *Principles of Optimal Design: Modeling and Computation*, 2nd ed., Cambridge University Press.

[33] Pontryagin, L. S., 2018, *Mathematical theory of optimal processes*, Routledge.

[34] Agulhari, C. M., Oliveira, R. C. L. F., and Peres, P. L. D., 2010, "Static output feedback control of polytopic systems using polynomial Lyapunov functions," *49th IEEE Conference on Decision and Control (CDC)*, pp. 6894–6901, doi: 10.1109/CDC.2010.5717214.

[35] Agulhari, C. M., Oliveira, R. C. L. F., and Peres, P. L. D., 2012, "LMI Relaxations for Reduced-Order Robust $\mathcal{H}_\infty$ Control of Continuous-Time Uncertain Linear Systems," IEEE Transactions on Automatic Control, **57**(6), pp. 1532–1537.

[36] Vargas, A. N., Agulhari, C. M., Oliveira, R. C. L. F., and Preciado, V. M., 2022, "Robust Stability Analysis of Linear Parameter-Varying Systems With Markov Jumps," IEEE Transactions on Automatic Control, **67**(11), pp. 6234–6239.

[37] Agulhari, C. M., Neto, J. M. M., Lacerda, M. J., de Souza, R. P. P., Castoldi, M. F., and Goedtel, A., 2021, "Robust real-time parameter estimation for linear systems affected by external noises and uncertainties," International Journal of Adaptive Control and Signal Processing, **35**(2), pp. 203–220.

[38] Andrade, L. H. S. d. and Agulhari, C. M., 2016, "Robust mixed $H_2/H\infty$ control of an nonlinear multivariable system," *2016 12th IEEE International Conference on Industry Applications (INDUSCON)*, IEEE, pp. 1–8, doi: 10.1109/INDUSCON.2016.7874550.

[39] Wu, J.-L., Yung, C.-F., and Lee, T.-T., 2016, "Simultaneous H∞ Control for a Collection of Nonlinear Systems in Strict-Feedback Form," *Nonlinear Systems*, D. Lee, T. Burg, and C. Volos, eds., IntechOpen, Rijeka, Chap. 9.

[40] Chilan, C. M., Herber, D. R., Nakka, Y. K., Chung, S.-J., Allison, J. T., Aldrich, J. B., and Alvarez-Salazar, O. S., 2017, "Co-Design of Strain-Actuated Solar Arrays for Spacecraft Precision Pointing and Jitter Reduction," AIAA Journal, **55**(9), pp. 3180–3195.

[41] Onoda, J. and Haftka, R. T., 1987, "An approach to structure/control simultaneous optimization for largeflexible spacecraft," AIAA Journal, **25**(8), pp. 1133–1138.

[42] Deshmukh, A. P. and Allison, J. T., 2016, "Multidisciplinary dynamic optimization of horizontal axis wind turbine design," Structural and Multidisciplinary Optimization, **53**(1), pp. 15–27.

[43] Cui, T., Allison, J. T., and Wang, P., 2019, "A Comparative Study of Formulations and Algorithms for Reliability-Based Co-Design Problems," Journal of Mechanical Design, **142**(3), p. 031104.

[44] Silva, E. B. d., Souza, R. P. P. d., Agulhari, C. M., Bressan, G. M., and Souza, W. A. d., 2024, "Robust State-Feedback Control and Convergence Analysis for Uncertain LPV Systems Using State and Parameter Estimation," Mathematics, **12**(13).

[45] Naidu, D., 2002, *Optimal Control Systems*, CRC Press, Inc.

[46] da Silva, J. G., Lacerda, M. J., Bertolin, A. L. J., Santos, J., and Nepomuceno, E., 2024, "LQR and Genetic Algorithms: An Effective Duo for Assessing Control Expenditure and Performance in Dynamic Systems," *2024 IEEE International Symposium on Circuits and Systems (ISCAS)*, pp. 1–5, doi: 10.1109/ISCAS58744.2024.10558029.

[47] Agulhari, C. M., Felipe, A., Oliveira, R. C. L. F., and Peres, P. L. D., 2019, "Algorithm 998: The Robust LMI Parser — A toolbox to construct LMI conditions for uncertain systems," ACM Transactions on Mathematical Software, **45**(3), p. 36:1–36:25.

[48] da Silva, J. G., Lacerda, M. J., Nazaré, T., Costa, M. M. G., Bertolin, A. L. J., and Nepomuceno, E., 2024, "Robust H_∞ Control Co-Design of Polytopic Systems," OSF.

[49] Ermakov, A. M., Ali, Z. A., Mahmoodi, K., Mason, O., and Ringwood, J. V., 2025, "Optimisation of heterogeneous wave energy converter arrays: A control co-design strategy," Renewable Energy, **244**, p. 122637.

[50] Peña-Sanchez, Y., García-Violini, D., Penalba, M., Zarketa-Astigarraga, A., Ferri, F., Nava, V., and Ringwood, J. V., 2024, "Control co-design for wave energy farms: Optimisation of array layout and mooring configuration in a realistic wave climate," Renewable Energy, **227**, p. 120506.